Carbohydrate Polymers 102 (2014) 151–158

Contents lists available at ScienceDirect

Carbohydrate Polymers

journal homepage: www.elsevier.com/locate/carbpol

Nanocrystalline chitin thin films

Chao Wang, Alan R. Esker*

Department of Chemistry, Virginia Tech, Blacksburg, VA 24061, United States

ARTICLE INFO

Article history:
Received 21 August 2013
Received in revised form 26 October 2013
Accepted 31 October 2013
Available online 15 November 2013

Keywords:
Chitin
Thin film
Chitinase
Bovine serum albumin
QCM-D
AFM

ABSTRACT

Elucidating the interactions between crystalline chitin and various biomacromolecules is of fundamental importance for designing and fabricating chitin-based biomaterials. This work highlights a simple method to prepare ultrathin films of chitin nanocrystals (chitin NC) by spincoating chitin NCs from a colloidal suspension onto a gold surface modified by an amine-terminated self-assembled monolayer. Atomic force microscopy confirmed that chitin NC films are reasonably smooth and homogeneous, and quartz crystal microbalance with dissipation monitoring (QCM-D) solvent exchange experiments demonstrated that chitin NC films have twice as much water as amorphous regenerated chitin (RChitin) films of similar thickness. QCM-D data also showed that chitinase-catalyzed hydrolysis of chitin NC films was much slower than that of RChitin films. Chitinase not only degraded, but also caused the swelling of the chitin nanocrystals. BSA adsorption studies demonstrated that chitin NC films have high protein loading capacity, and thus show potential applications for enzyme immobilization.

1. Introduction

As the second most abundant biopolymer in nature, chitin is widely distributed in the exoskeletons of crustaceans (e.g. shrimps, crabs and lobsters) and insects, the cell walls of fungi, and the beaks of cephalopods (e.g. octopi and squid) (Rinaudo, 2006). In nature, chitin occurs as ordered crystalline microfibrils which associate with other materials, such as proteins, lipids, polysaccharides, calcium carbonate, and pigments to form natural composites (Goodrich & Winter, 2007). Two polymorphs of chitin (α and β) have been reported, differing with respect to the locations and quantity of hydrogen bonds (Muzzarelli, 2012; Zeng, He, Li, & Wang, 2012). α-Chitin is the most abundant and stable form, and it is derived from crustacean tendons and shells, yeast and fungal cell walls, as well as insect cuticles (Muzzarelli, 2011; Muzzarelli et al., 2012). β-Chitin is less abundant and stable than α-chitin, and it is found in squid pens and tubeworms (Blackwell, Parker, & Rudall, 1965; Rudall & Kenchington, 1973). Compared to α-chitin, β-chitin is more susceptible to swelling. β-Chitin can be reversibly swelled by water, alcohols or amines, and irreversibly swelled by strongly acidic or basic solutions (Saito, Putaux, Okano, Gaill, & Chanzy, 1997; Saito, Okano, Gaill, Chanzy, & Putaux, 2000). β-Chitin could also be converted to thermodynamically stable α-chitin via dissolution or extensive swelling under strongly acidic or basic conditions (Noishiki et al., 2003; Saito et al., 1997). Due to its biocompatibility, biodegradability, affinity for proteins, antimicrobial and gel-forming properties, chitin is widely used in the medical and pharmaceutical area, such as wound-dressing materials (Jayakumar, Prabaharan, Sudheesh Kumar, Nair, & Tamura, 2011; Kumar et al., 2010; Muzzarelli, 2009), drug carriers (Mi et al., 2003; Rejinold, Chennazhi, Tamura, Nair, & Rangasamy, 2011), tissue engineering scaffolds (Freier, Montenegro, Shan Koh, & Shoichet, 2005; Noh et al., 2006), enzyme and cell immobilization supports (Krajewska, 2004; Muzzarelli, 1980), and biosensors (Ohashi & Karube, 1995; Ohashi & Koriyama, 1992).

Fundamental knowledge of the interactions between chitin and proteins, polysaccharides, calcium carbonate, enzymes, drugs, cells and synthetic materials is not only important for elucidating biological processes associated with chitin, but also for designing novel chitin-based biomaterials. Model chitin surfaces and the development of surface characterization techniques provide a convenient way to study and quantify these interactions. Recently, our group reported a simple method to prepare homogeneous, smooth and ultrathin chitin films by spincoating trimethylsilyl chitin (TMS-Chitin) from a mixture of chloroform and tetrachloroethane onto silica or gold surfaces. These TMSChitin films were subsequently regenerated to amorphous chitin upon exposure to the vapor of a hydrochloric acid solution. The regenerated chitin thin films were used as a model surface to study the interactions between chitin and bovine serum albumin (BSA) via a quartz crystal microbalance with dissipation monitoring (QCM-D), surface plasmon resonance (SPR) and atomic force microscopy (AFM) (Kittle et al., 2012), as well as chitinases (Wang, Kittle, Qian, Roman, & Esker, 2013). However, the regenerated chitin films are only representative of amorphous chitin structures, differing in crystallinity from native chitin.

* Corresponding author at: Department of Chemistry (0212), Virginia Tech, Blacksburg, VA 24061, United States. Tel.: +1 540 231 4601; fax: +1 540 231 3255.
E-mail addresses: cwang09@vt.edu (C. Wang), aesker@vt.edu (A.R. Esker).

0144-8617/$ – see front matter © 2013 Elsevier Ltd. All rights reserved.
http://dx.doi.org/10.1016/j.carbpol.2013.10.103

Crystalline chitin thin films are expected to provide a better model to study the enzymatic degradation of native chitin, chitin–protein interactions, fungal cell wall component interactions and biomineralization.

Various cellulose model thin films (including both amorphous and crystalline) have been prepared via spincoating or the Langmuir–Blodgett techniques (Ahola, Salmi, Johansson, Laine, & Österberg, 2008; Edgar & Gray, 2003; Eriksson et al., 2005; Fält, Wågberg, Vesterlind, & Larsson, 2004; Gunnars, Wågberg, & Cohen Stuart, 2003; Habibi, Foulon, Aguié-Béghin, Molinari, & Douillard, 2007; Kontturi, Thüne, & Niemantsverdriet, 2003; Kontturi, Tammelin, & Osterberg, 2006; Maren, 2009; Schaub, Wenz, Wegner, Stein, & Klemm, 1993; Yokota, Kitaoka, Sugiyama, & Wariishi, 2007). Edgar and Gray (2003) reported the preparation of smooth cellulose nanocrystalline thin films by spincoating colloidal suspensions of cellulose nanocrystals onto mica surfaces. Habibi et al. (2007) prepared monolayers of cellulose nanocrystals via the Langmuir–Blodgett technique.

Similar to cellulose, native chitin is highly crystalline with some disordered or paracrystalline regions that arise from defects. The disordered or paracrystalline regions are preferentially hydrolyzed or oxidized under certain conditions, whereas crystalline regions remain intact. Thus, rod-like chitin nanocrystals (chitin NCs) or whiskers can be produced (Habibi, Lucia, & Rojas, 2010; Zeng et al., 2012). Chitin NCs are normally prepared by hydrolysis of chitin in hydrochloric acid solutions (Goodrich & Winter, 2007; Tzoumaki, Moschakis, & Biliaderis, 2010; Zeng et al., 2012). The sizes of the chitin NCs are greatly affected by the origin of the chitin, concentration of the hydrochloric acid solutions and the hydrolysis time, with the lengths varying over the range of 150–2200 nm, and the widths over the range of 10–50 nm (Zeng et al., 2012). Recently, Fan, Saito, and Isogai (2008) prepared chitin NCs via 2,2,6,6-tetramethylpiperidine-1-oxyl radical (TEMPO) mediated oxidation of α-chitin with NaClO as a co-oxidant. The resulting rod-like nanocrystals had high surface charges because some hydroxyl groups on the surface were oxidized to carboxylate groups, and the average nanocrystal length and width were 340 nm and 8 nm, respectively.

This work presents a simple method to prepare smooth and ultrathin nanocrystalline chitin films. The morphologies, surface roughnesses, thicknesses and water contents of these films were characterized via atomic force microscopy (AFM), ellipsometry and a quartz crystal microbalance with dissipation monitoring (QCM-D). The chitinase-catalyzed hydrolysis of these chitin films was investigated via QCM-D. The utility of these chitin films as potential enzyme immobilization supports was demonstrated through the adsorption of bovine serum albumin (BSA) onto the films in QCM-D studies.

2. Experimental

2.1. Materials

α-Chitin from shrimp shells (practical grade, >95% acetylated) was purchased from Sigma–Aldrich. The TMSChitin (degree of substitution = 2.0) was synthesized as previously described (Kittle et al., 2012; Kurita, Sugita, Kodaira, Hirakawa, & Yang, 2005). Colloidal suspensions of chitin NC were prepared through a HCl hydrolysis procedure reported by Goodrich and Winter (2007). Chitinase (from *Streptomyces griseus*, lyophilized powder, ≥200 units/g solid) is an extracellular enzyme complex (Berger & Reynold, 1958) with a molar mass of ~30 kDa and was purchased from Sigma–Aldrich. Bovine serum albumin (lyophilized powder) was purchased from Sigma–Aldrich and used as received. 11-Amino-1-undecanethiol was purchased from Fisher Scientific and used as received. Sodium phosphate monobasic monohydrate and sodium phosphate dibasic heptahydrate were purchased from Sigma–Aldrich and used as received to prepare buffer solutions (pH 6.0). Hydrochloric acid (37.3%) was purchased from Fisher Scientific. Hydrogen peroxide (30%, w/w), sulfuric acid (conc.), and ammonium hydroxide (28%, w/w) were used to clean the surfaces and were purchased from EM Science, VWR International, and Fisher Scientific, respectively. All other chemicals and solvents were obtained from Fisher Scientific and used as received. Ultrapure water with a resistivity of 18 MΩ cm and <5 ppb inorganic impurities was used in all experiments (Milli-Q Gradient A-10, Millipore).

2.2. Surface preparation

Surface cleaning. Silica coated QCM-D sensors (Q-Sense AB, QSX-303, 5 MHz) were cleaned prior to use by immersion into a 7:3 (v/v) solution of sulfuric acid:hydrogen peroxide, followed by a rinse with ultrapure water and drying with nitrogen. Gold coated QCM-D sensors (Q-Sense AB, QSX-301, 5 MHz) were cleaned prior to use by exposure to UV/ozone for 20 min, immersion into a 1:1:5 (v/v/v) solution of ammonium hydroxide:hydrogen peroxide:water at 80 °C for 1 h, a rinse with ultrapure water and drying with nitrogen.

Amorphous regenerated chitin (*RChitin*) *films*. The details of the preparation and characterization of the smooth and amorphous chitin films was previously published (Kittle et al., 2012). The TMS-Chitin was dissolved in a chloroform/tetrachloroethane (4:1, v/v) mixture to form 0.6% TMSChitin solutions by mass. These solutions were filtered through a 0.45 μm syringe filter (VWR PTFE) to remove dust particles and aggregates. The filtered solutions were spincoated onto silica coated QCM-D sensors at a spinning speed of 3000 rpm for 1 min and regenerated to amorphous chitin by exposure of these surfaces to the vapor of 10% by mass aqueous hydrochloric acid solution to obtain RChitin films with thicknesses of ~20 nm.

Nanocrystalline chitin films. A SAM-NH_2 was formed on a cleaned gold QCM-D sensor crystal after immersion in a 1 mM solution of 11-amino-1-undecanol in ethanol for 24 h. Films of chitin NC with different thicknesses were obtained by spincoating at 4000 rpm for 1 min from colloidal suspensions of chitin NCs with concentrations that ranged from 0.50% to 2.20% by mass. Films were then dried overnight at 70 °C before thicknesses were determined.

2.3. AFM measurements

All the surfaces were imaged in tapping mode with an Asylum Research AFM (MFP-3D-BIO, Asylum Research). Height images were collected under ambient conditions (22 °C, 50% humidity) using a silicon tip (OMCL-AC160TS, Olympus Corp.). The reported roughnesses were determined from the root mean square (RMS) values of 2 μm × 2 μm, 5 μm × 5 μm, or 10 μm × 10 μm scan areas. In order to observe the morphology of chitin NCs, chitin NCs were deposited onto SAM-NH_2 coated gold surfaces through spincoating of an aqueous 0.005% by mass chitin NC suspension at 4000 rpm for 1 min. The samples were then dried overnight at 70 °C before imaging.

2.4. XRD measurements

X-ray diffraction patterns of lyophilized chitin NCs, raw α-chitin and regenerated chitin powders were obtained on a Rigaku Mini-Flex II Desktop X-Ray Diffractometer. The radiation source was Cu(Kα) radiation with a wavelength of 1.54 Å. The angular scanning range was 2θ = 5–50° with 0.01° steps.

2.5. Ellipsometry measurements

Ellipsometry measurements of RChitin and chitin NC films were conducted at multiple-angles-of-incidence (60–80°, 1° steps) using a He:Ne laser at a constant wavelength of 632.8 nm (Picometer Ellipsometer, Beaglehole Instruments). The thicknesses of the films were deduced from modeling with TFCompanion software (Semiconsoft) with an assumption of a refractive index of 1.51 for both RChitin and chitin NCs (Kittle et al., 2012; Montiel-González, Luna-Bárcenas, & Mendoza-Galván, 2008).

2.6. QCM-D measurements

An E4 quartz crystal microbalance with dissipation monitoring (Q-Sense AB) was used to study the water content of the chitin films, the enzymatic degradation of the chitin films in the presence of chitinase, and the adsorption of BSA onto the chitin films. Frequency (Δf) and dissipation (ΔD) changes for the fundamental frequency (4.95 MHz for both silica coated quartz crystals) and six odd overtones (n = 3–13) were monitored simultaneously during the QCM-D measurements. Curves from the fifth overtone (n = 5) are used as representative curves for all of the graphs.

Water content. The water content of chitin NC films was determined using a H_2O/D_2O solvent exchange procedure as previously reported (Kittle et al., 2011, 2012).

Enzymatic degradation. The QCM-D sensor was placed in a flow cell and allowed to equilibrate for 1 h in pH 6.0 phosphate buffer to obtain a flat baseline at 37 °C. Chitinase solutions (1.0 mL) were then flowed over the surface at a rate of 0.100 mL min^{-1}. The flow was stopped and the measurements were made in the absence of flow. At the end of the measurement, buffer was typically flowed through the system for the removal of residual and reversibly adsorbed enzyme and products.

BSA adsorption. The QCM-D sensor was placed in a flow cell and allowed to equilibrate for 1 h in water at 25 °C until a flat baseline was obtained. Solutions of BSA in ultrapure water (100 mg L^{-1}) were then introduced for ~25 min at the rate of 0.200 mL min^{-1}, followed by a rinse with ultrapure water for ~10 min.

For QCM-D measurements, if the adsorbed mass is evenly distributed, rigidly attached, and small compared to the mass of the crystal, surface concentration (Γ_{QCM}), can be calculated from the Sauerbrey equation (Sauerbrey, 1959):

$$\Gamma_{QCM} = -C\left(\frac{\Delta f}{n}\right) \quad (1)$$

where n is the overtone number and C is a constant (0.177 mg m^{-2} Hz^{-1}). However, the linear relationship between the adsorbed mass and the scaled frequency change ($\Delta f/n$) is not valid for viscoelastic layers adsorbed onto the solid surfaces. By measuring the dissipation of energy in the adsorbed layers simultaneously with the frequency change, information is obtained about the rigidity/softness of the adsorbed layer. The dissipation factor is defined as a ratio between the energy dissipated and the energy stored during a single oscillation (Dixon, 2008).

$$D = \frac{E_{dissipated}}{2\pi E_{stored}} \quad (2)$$

3. Results and discussion

3.1. Characterization of chitin NCs

The morphology of chitin NCs on gold surfaces modified by SAM-NH_2 was observed by AFM, and a height image is provided in Fig. 1. The rod-like nanocrystals are well dispersed on the surface with lengths and widths ranging from 200 to 600 nm and

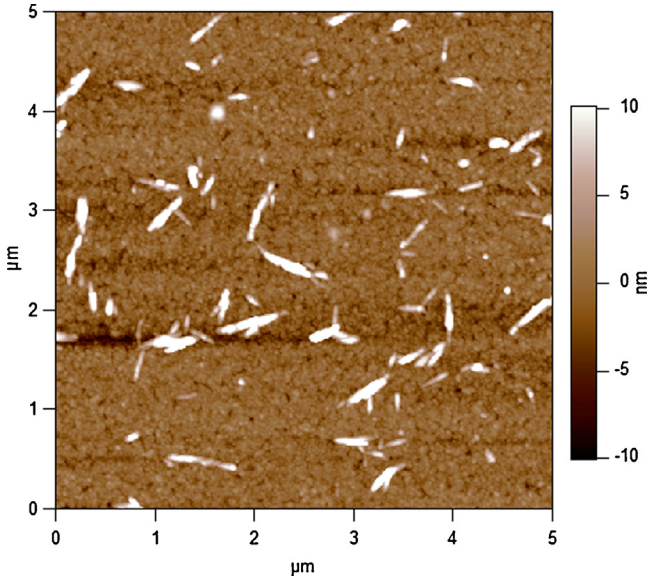

Fig. 1. A representative 5 µm × 5 µm AFM height image of chitin NCs on a SAM-NH_2 coated gold surface.

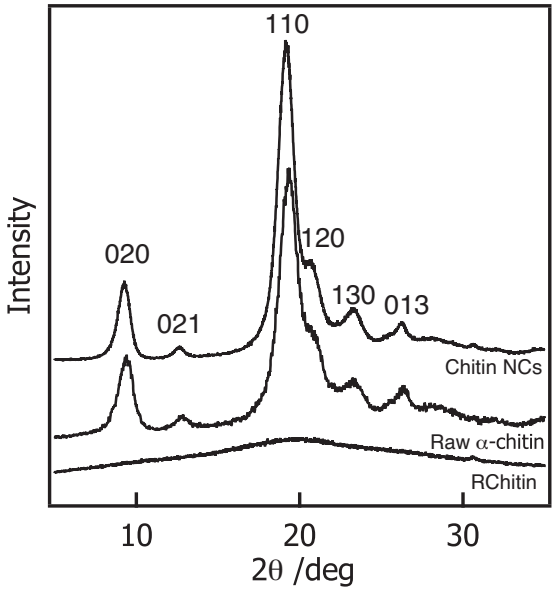

Fig. 2. Powder X-ray diffraction data for chitin NCs, raw α-chitin, and RChitin.

30 to 70 nm, respectively. Goodrich and Winter (2007) used the same procedure to prepare chitin NCs, and used transmission electron microscopy to determine the nanocrystals had lateral and transverse dimensions of 200–500 nm and 10–15 nm, respectively. They also found that HCl hydrolysis had little effect on the degree of *N*-acetylation via solid-state CP-MAS ^{13}C NMR spectra, and Congo red dye adsorption experiments showed higher surface areas (347 m^2 g^{-1}) for chitin NCs than the original chitin fiber, as well as cellulose nanocrystals prepared by sulfuric acid hydrolysis (Goodrich & Winter, 2007).

The diffraction patterns of lyophilized chitin NCs, RChitin and raw α-chitin prior to hydrolysis are shown in Fig. 2. Both chitin NCs and raw α-chitin show the typical reflections of pure α-chitin, corresponding to the 020, 021, 110, 120, 130, and 013 crystallographic planes (Goodrich & Winter, 2007; Minke & Blackwell, 1978). In contrast, the absence of the characteristic diffraction peaks for RChitin indicated that RChitin is mostly unoriented and amorphous.

Crystallinity index (*CI*) has been used for the interpretation of changes in chitosan and chitin crystal structure during physicochemical treatments (Schiffman, Stulga, & Schauer, 2009; Zhang, Xue, Li, Zhang, & Fu, 2006). Percentage values of *CI* can be calculated from:

$$\text{Crystallinity index } (CI)\ (\%) = \left[\frac{I_{110} - I_{\text{am}}}{I_{110}}\right] \times 100 \quad (3)$$

where I_{110} (arbitrary units) is the maximum intensity of the 110 peak at $2\theta = 19^\circ$, and I_{am} (arbitrary units) is the maximum intensity of the amorphous diffraction at $2\theta = 12.6^\circ$. The *CI* increased from ~91% (raw α-chitin) to ~97% (chitin NCs), indicating that some of the amorphous regions in raw α-chitin were digested during HCl hydrolysis.

3.2. Preparation of chitin NC films

Chitin NC films with different thicknesses were obtained by spincoating from aqueous colloidal chitin NC suspensions (0.50–2.20% by mass) onto gold surfaces modified by SAM-NH_2. Height images from AFM of chitin NC films (~20 nm thick) spincoated from an aqueous 1.80% by mass chitin NC colloidal suspensions are shown in Fig. 3. The chitin NC films are reasonably smooth and homogeneous; however, the rod-like features are clearly present in the AFM images. The chitin NC films have RMS roughnesses of ~6.4 nm for the 10 μm × 10 μm and ~6.1 nm for the 2 μm × 2 μm scan area. These roughnesses are slightly larger than those reported for cellulose nanocrystal films (e.g. ~5.3 nm for sulfated cellulose nanocrystal (SNC) films on silicon wafers (Lefebvre & Gray, 2005), ~1.5 nm for SNC films on SAM-NH_2 coated gold surfaces (Kittle et al., 2011), and ~2.5 nm for solvolytically desulfated cellulose nanocrystal films on gold surfaces modified by SAM-NH_2 (Kittle et al., 2011)). The relatively larger roughnesses for chitin NC films are likely a consequence of the larger size of the chitin NCs relative to the cellulose nanocrystals (Jiang, Esker, & Roman, 2010).

3.3. Water content of chitin NC films

The water content of chitin NC films was studied using QCM-D and a previously reported H_2O/D_2O solvent exchange procedure (Kittle et al., 2011). A chitin NC film coated QCM-D sensor was exposed to H_2O until a stable baseline was obtained, and then H_2O was switched to D_2O. A change of $\Delta f/n$ was observed that arose from the different physical properties (density, viscosity and molar mass) of the two solvents. The mass of water associated with the film (Γ_{water}) was calculated from the change in $\Delta f/n$ associated with switching from H_2O to D_2O using Eq. (1) (Kittle et al., 2011). The water contents of chitin NC and RChitin films as a function of film thickness are shown in Fig. 4. A linear fit of the chitin NC data gave a slope of $2.50 \pm 0.03\ \text{mg m}^{-2}\ \text{nm}^{-1}$, whereas a linear fit of the RChitin data gave a slope of $1.19 \pm 0.05\ \text{mg m}^{-2}\ \text{nm}^{-1}$. Therefore, chitin NC films had twice as much water as RChitin films of the same thicknesses. These slopes were converted into a mass percentages of water through the same procedure employed by Kittle et al. (2011) for cellulose films under the assumption that a chitin monolayer has the same surface concentration ($\Gamma_{\text{monolayer}} = 0.45\ \text{mg m}^{-2}$) (Kawaguchi, Nakahara, & Fukuda, 1985) and thickness (0.36 nm) (Schaub et al., 1993) as a cellulose monolayer. This conversion yielded 67 ± 1% water by mass within the chitin NC films versus 49 ± 2% water by mass previously deduced for RChitin films (Kittle et al., 2012). As was the case for nanocrystalline cellulose versus regenerated cellulose films (Kittle et al., 2011), this difference is attributed to the voids between individual chitin NCs in chitin NC films, whereas RChitin films are not porous (Kittle et al., 2012).

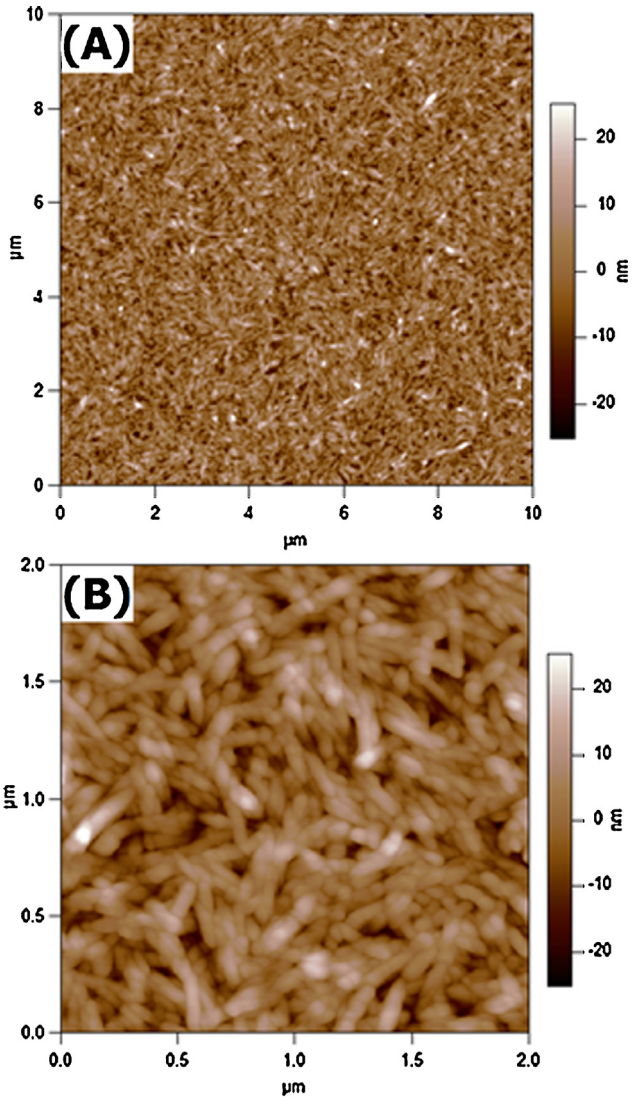

Fig. 3. (A) 10 μm × 10 μm and (B) 2 μm × 2 μm AFM height images of chitin NC films on gold surfaces modified by SAM-NH_2. The RMS roughnesses for the images are: (A) ~6.4 nm and (B) ~6.1 nm.

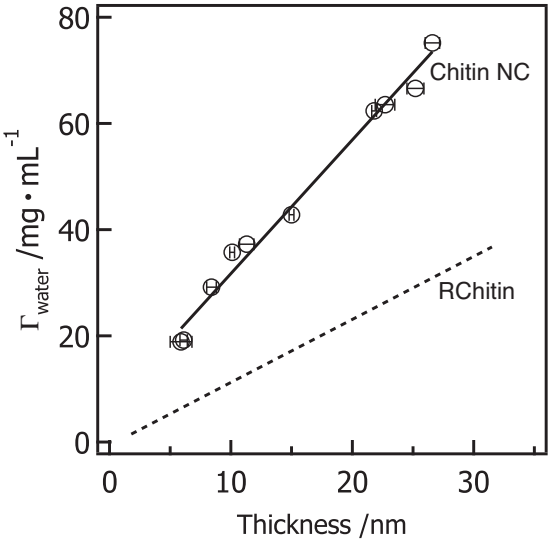

Fig. 4. Γ_{water} versus film thickness for (○,—) chitin NC and (----) RChitin (Kittle et al., 2012) films. Typical, one standard deviation error bars are comparable to the size of the symbols of chitin NC.

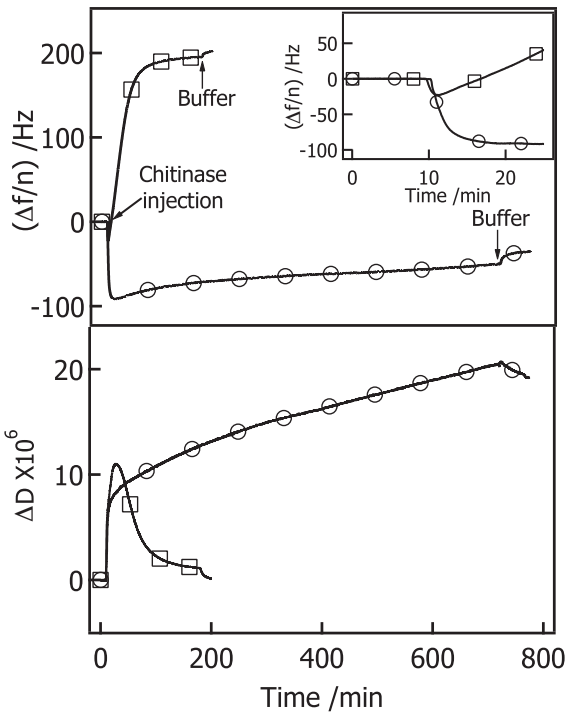

Fig. 5. Representative $\Delta f/n$ and ΔD versus time for chitinase (0.5 mg mL^{-1}) activity on (○) chitin NC and (□) RChitin films at 37 °C in a 50 mM phosphate buffer (pH 6.0). Curves correspond to the fifth overtone. The inset highlights the region of the $\Delta f/n$ profile dominated by chitinase adsorption onto the chitin films.

3.4. Enzymatic degradation of nanocrystalline and amorphous chitin films

Crystallinity is one of the most important factors that affects the enzymatic degradation of both natural and synthetic polymers (Ahola, Turon, Österberg, Laine, & Rojas, 2008; Cai, Dave, Gross, & McCarthy, 1996; Fan, Lee, & Beardmore, 1980; Hall, Bansal, Lee, Realff, & Bommarius, 2010; Kikkawa, Abe, Iwata, Inoue, & Doi, 2002; Kumagai, Kanesawa, & Doi, 1992; Lee, Kim, Ryu, & Taguchi, 1983). Recently, our group successfully prepared smooth and homogeneous RChitin thin films (Kittle et al., 2012), and studied the enzymatic degradation of the amorphous RChitin films in the presence of chitinase (from *S. griseus*) at various conditions via QCM-D and AFM (Wang et al., 2013). The combination of RChitin and chitin NC films provided a good model for the investigation of the effects of crystallinity on the enzymatic degradation of chitin. Fig. 5 contains QCM-D data for the enzymatic degradation of RChitin and chitin NC films. As seen in Fig. 5, the $\Delta f/n$ profile indicated that the RChitin film (with an initial thickness of ~20 nm) was hydrolyzed quickly (total hydrolysis in ~80 min) as previously reported (Wang et al., 2013). Also as previously reported (Wang et al., 2013), the dissipation initially increased as chitinase adsorbed onto the film and continued to increase as the chitinase penetrated into the RChitin film. The subsequent drop in ΔD arose from the exhaustion of the chitin substrate and subsequent chitinase desorption from the film. In contrast, the $\Delta f/n$ profile for chitin NC film revealed much slower hydrolysis with degradation of only a portion of the chitin NC film (also with an initial thickness of ~20 nm) after 12 h incubation with chitinase. The larger initial $\Delta f/n$ decrease for the chitin NC film relative to the RChitin film in the inset of Fig. 5 indicated that the amount of chitinase adsorbed onto the chitin NC film was greater than that adsorbed onto the RChitin film. This behavior was attributed to the voids within the chitin NC film or put another way, an effectively larger accessible surface area. The adsorption of chitinase onto and within the chitin NC film was accompanied by an instantaneous ΔD increase. With time, ΔD grew, however, the rate of growth decreased considerably. One possible explanation for the ΔD profile is that endochitinase in the chitinase complex disrupted the hydrogen bonds and caused swelling of the chitin nanocrystals (Jollès & Muzzarelli, 1999). Similar behavior has been observed for cellulases. Like chitinase, cellulase is also an enzyme complex composed of endoglucanases, exoglucanases and cellobiase (Ahola, Turon, et al., 2008). Josefsson, Henriksson, and Wågberg (2008) studied the functions of different pure cellulases on model cellulose films via QCM-D, and concluded that endoglucanases not only produced new end groups, but also caused swelling of the cellulose films. Similar behavior was also reported by Cheng et al. (2011, 2012).

Faster hydrolysis of amorphous chitin films than chitin NC films is also consistent with other studies of enzymatic degradation of semi-crystalline polymers. Various studies have shown that amorphous cellulose was hydrolyzed much faster than crystalline cellulose. In partially crystalline cellulose samples, the amorphous domains were hydrolyzed first, and left the crystalline domains which underwent slower degradation (Ahola, Turon, et al., 2008; Fan et al., 1980; Hall et al., 2010; Lee et al., 1983). The enzymatic degradation of polyesters has also been widely investigated for their applications as biomaterials (Cai et al., 1996; Kikkawa et al., 2002; Kumagai et al., 1992). Cai et al. (1996) studied the proteinase K-catalyzed degradation of poly(1actic acid), and Kumagai et al. (1992) studied the enzymatic degradation of poly(3-hydroxybutyrate) (PHB) in the presence of PHB depolymerase (from *Alcaligenes faecalis*). Both of these studies found that the degradation rate of polyesters decreased with increasing crystallinity of the polymer, and the enzymes hydrolyzed the amorphous domains before the crystalline domains (Cai et al., 1996; Kumagai et al., 1992).

3.5. Adsorption of BSA onto chitin NC films

As a biocompatible and biodegradable natural material, chitin is a good support for enzyme immobilization, and thus shows potential applications in biological sensing and biocatalysis (Krajewska, 2004; Muzzarelli, 1980; Ohashi & Karube, 1995; Ohashi & Koriyama, 1992). Our group used BSA as a model protein for a study of the interactions between RChitin films and proteins, and showed that BSA formed a monolayer ($\Gamma_{\text{QCM-D}} = 3.6 \pm 0.1$ mg m^{-2}) on RChitin surfaces (Kittle et al., 2012). The value of $\Gamma_{\text{QCM-D}}$ for BSA adsorption onto RChitin films was independent of film thickness. Higher BSA loading because of a large accessible surface area for the porous chitin NC films was expected. Data from QCM-D studies of BSA adsorption onto chitin NC films with different thicknesses are provided in Fig. 6. Compared to RChitin film, BSA showed stronger adsorption onto chitin NC films than RChitin films, and the amount of adsorption was dependent upon the film thickness. The adsorption of BSA onto chitin NC films with a film thickness of 13.7 ± 0.8 nm yielded $\Delta f/n = -75 \pm 2$ Hz via QCM-D, or $\Gamma_{\text{QCM-D}} = 13.3 \pm 0.4$ mg m^{-2} according to Eq. (1). For a thicker chitin NC film (16.8 ± 0.5 nm), $\Gamma_{\text{QCM-D}}$ increased to 15.0 ± 0.5 mg m^{-2}. After rinsing with water, the amount of BSA on the chitin NC films was not significantly different from the amount of BSA present prior to rinsing (i.e. BSA adsorption was irreversible). These results were consistent with porous chitin NC films. Furthermore, ΔD profiles in Fig. 6 almost instantaneously plateaued after the injection of BSA solution. These ΔD changes associated with BSA adsorption are much smaller than those observed for chitinase adsorption (Fig. 5) and did not grow with time. These results show that protein adsorption alone is insufficient to swell the chitin NC film and that the ΔD profile in Fig. 5 is a consequence of both adsorption and catalytic activity.

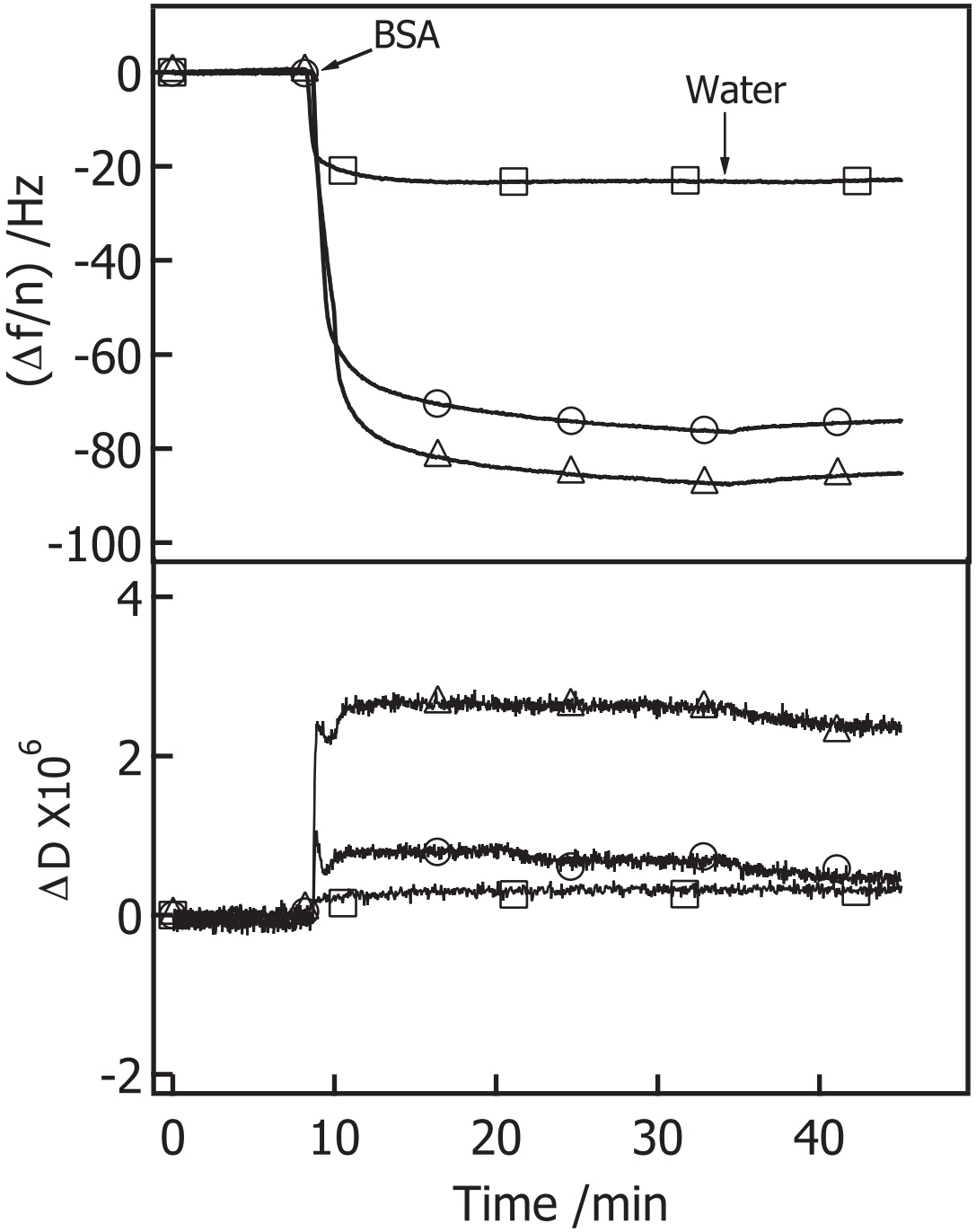

Fig. 6. Representative $\Delta f/n$ and ΔD versus time for BSA (100 mg L^{-1}) adsorption onto (□) RChitin, (○) chitin NC (13.7 ± 0.8 nm) and (△) chitin NC (16.8 ± 0.5 nm) films at 25 °C. Curves correspond to the fifth overtone.

4. Conclusions

This work provides a simple method for the preparation of nanocrystalline chitin thin films by spincoating from aqueous colloidal chitin nanocrystal suspensions onto SAM-NH_2 coated gold surfaces. The morphology and crystallinity index of the chitin nanocrystals were determined by AFM and XRD. Images obtained from AFM confirmed that chitin NC films were reasonably smooth and homogeneous, while QCM-D solvent exchange experiments demonstrated that chitin NC films had twice as much water as RChitin films of similar thickness. Data for the enzymatic degradation of chitin NC films from QCM-D revealed much slower hydrolysis of chitin NC films than amorphous RChitin films. The ΔD profile from QCM-D was consistent with a chitinase induced enhancement of the swelling of the chitin NC film. Studies of BSA adsorption onto chitin NC films showed chitin NC films had higher protein loading capacities than RChitin films, an indication that chitin NC films have potential as biocompatible supports for biological sensors and catalysts.

Acknowledgments

C.W. and A.R.E. were supported in part by the Center for LignoCellulose Structure and Formation, an Energy Frontier Research

Center funded by the U.S. Department of Energy, Office of Science, Office of Basic Energy Sciencesunder Award Number DE-SC0001090. We are grateful to Robert B. Moore's and Maren Roman's groups at Virginia Tech for the help on the XRD and AFM measurements.

References

Ahola, S., Salmi, J., Johansson, L. S., Laine, J., & Österberg, M. (2008). Model films from native cellulose nanofibrils. Preparation, swelling, and surface interactions. *Biomacromolecules*, *9*(4), 1273–1282.

Ahola, S., Turon, X., Österberg, M., Laine, J., & Rojas, O. J. (2008). Enzymatic hydrolysis of native cellulose nanofibrils and other cellulose model films: Effect of surface structure. *Langmuir*, *24*(20), 11592–11599.

Berger, L. R., & Reynold, D. M. (1958). The chitinase system of a strain of *Streptomyces griseus*. *Biochimica et Biophysica Acta*, *29*(3), 522–534.

Blackwell, J., Parker, K. D., & Rudall, K. M. (1965). Chitin in pogonophore tubes. *Journal of the Marine Biological Association of the United Kingdom*, *45*(03), 659–661.

Cai, H., Dave, V., Gross, R. A., & McCarthy, S. P. (1996). Effects of physical aging, crystallinity, and orientation on the enzymatic degradation of poly(lactic acid). *Journal of Polymer Science Part B: Polymer Physics*, *34*(16), 2701–2708.

Cheng, G., Datta, S., Liu, Z., Wang, C., Murton, J. K., Brown, P. A., et al. (2012). Interactions of endoglucanases with amorphous cellulose films resolved by neutron reflectometry and quartz crystal microbalance with dissipation monitoring. *Langmuir*, *28*(22), 8348–8358.

Cheng, G., Liu, Z., Murton, J. K., Jablin, M., Dubey, M., Majewski, J., et al. (2011). Neutron reflectometry and QCM-D study of the interaction of cellulases with films of amorphous cellulose. *Biomacromolecules*, *12*(6), 2216–2224.

Dixon, M. C. (2008). Quartz crystal microbalance with dissipation monitoring: Enabling real-time characterization of biological materials and their interactions. *Journal of Biomolecular Techniques*, *19*(3), 151–158.

Edgar, C., & Gray, D. (2003). Smooth model cellulose I surfaces from nanocrystal suspensions. *Cellulose*, *10*(4), 299–306.

Eriksson, J., Malmsten, M., Tiberg, F., Callisen, T. H., Damhus, T., & Johansen, K. S. (2005). Enzymatic degradation of model cellulose films. *Journal of Colloid and Interface Science*, *284*(1), 99–106.

Fält, S., Wågberg, L., Vesterlind, E. L., & Larsson, P. T. (2004). Model films of cellulose ID – Improved preparation method and characterization of the cellulose film. *Cellulose*, *11*(2), 151–162.

Fan, L. T., Lee, Y.-H., & Beardmore, D. H. (1980). Mechanism of the enzymatic hydrolysis of cellulose: Effects of major structural features of cellulose on enzymatic hydrolysis. *Biotechnology and Bioengineering*, *22*(1), 177–199.

Fan, Y., Saito, T., & Isogai, A. (2008). Chitin nanocrystals prepared by TEMPO-mediated oxidation of α-chitin. *Biomacromolecules*, *9*(1), 192–198.

Freier, T., Montenegro, R., Shan Koh, H., & Shoichet, M. S. (2005). Chitin-based tubes for tissue engineering in the nervous system. *Biomaterials*, *26*(22), 4624–4632.

Goodrich, J. D., & Winter, W. T. (2007). α-Chitin nanocrystals prepared from shrimp shells and their specific surface area measurement. *Biomacromolecules*, *8*(1), 252–257.

Gunnars, S., Wågberg, L., & Cohen Stuart, M. A. (2003). Corrigendum: Model films of cellulose: I. Method development and initial results. *Cellulose*, *10*(2), 185.

Habibi, Y., Foulon, L., Aguié-Béghin, V., Molinari, M., & Douillard, R. (2007). Langmuir–Blodgett films of cellulose nanocrystals: Preparation and characterization. *Journal of Colloid and Interface Science*, *316*(2), 388–397.

Habibi, Y., Lucia, L. A., & Rojas, O. J. (2010). Cellulose nanocrystals: Chemistry, self-assembly, and applications. *Chemical Reviews*, *110*(6), 3479–3500.

Hall, M., Bansal, P., Lee, J. H., Realff, M. J., & Bommarius, A. S. (2010). Cellulose crystallinity – A key predictor of the enzymatic hydrolysis rate. *FEBS Journal*, *277*(6), 1571–1582.

Jayakumar, R., Prabaharan, M., Sudheesh Kumar, P. T., Nair, S. V., & Tamura, H. (2011). Biomaterials based on chitin and chitosan in wound dressing applications. *Biotechnology Advances*, *29*(3), 322–337.

Jiang, F., Esker, A. R., & Roman, M. (2010). Acid-catalyzed and solvolytic desulfation of H_2SO_4-hydrolyzed cellulose nanocrystals. *Langmuir*, *26*(23), 17919–17925.

Jollès, P., & Muzzarelli, R. A. A. (Eds.). (1999). *Chitin and chitinases*. Basel: Birkhäuser.

Josefsson, P., Henriksson, G., & Wågberg, L. (2008). The physical action of cellulases revealed by a quartz crystal microbalance study using ultrathin cellulose films and pure cellulases. *Biomacromolecules*, *9*(1), 249–254.

Kawaguchi, T., Nakahara, H., & Fukuda, K. (1985). Monomolecular and multimolecular films of cellulose esters with various alkyl chains. *Thin Solid Films*, *133*(1–4), 29–38.

Kikkawa, Y., Abe, H., Iwata, T., Inoue, Y., & Doi, Y. (2002). Crystallization, stability, and enzymatic degradation of poly(L-lactide) thin film. *Biomacromolecules*, *3*(2), 350–356.

Kittle, J. D., Du, X., Jiang, F., Qian, C., Heinze, T., Roman, M., et al. (2011). Equilibrium water contents of cellulose films determined via solvent exchange and quartz crystal microbalance with dissipation monitoring. *Biomacromolecules*, *12*(8), 2881–2887.

Kittle, J. D., Wang, C., Qian, C., Zhang, Y., Zhang, M., Roman, M., et al. (2012). Ultrathin chitin films for nanocomposites and biosensors. *Biomacromolecules*, *13*(3), 714–718.

Kontturi, E., Tammelin, T., & Osterberg, M. (2006). Cellulose-model films and the fundamental approach. *Chemical Society Reviews*, *35*(12), 1287–1304.

Kontturi, E., Thüne, P. C., & Niemantsverdriet, J. W. (2003). Cellulose model surfacessimplified preparation by spin coating and characterization by x-ray photoelectron spectroscopy, infrared spectroscopy, and atomic force microscopy. *Langmuir*, *19*(14), 5735–5741.

Krajewska, B. (2004). Application of chitin- and chitosan-based materials for enzyme immobilizations: A review. *Enzyme and Microbial Technology*, *35*(2–3), 126–139.

Kumagai, Y., Kanesawa, Y., & Doi, Y. (1992). Enzymatic degradation of microbial poly(3-hydroxybutyrate) films. *Die Makromolekulare Chemie*, *193*(1), 53–57.

Kumar, P. T. S., Abhilash, S., Manzoor, K., Nair, S. V., Tamura, H., & Jayakumar, R. (2010). Preparation and characterization of novel β-chitin/nanosilver composite scaffolds for wound dressing applications. *Carbohydrate Polymers*, *80*(3), 761–767.

Kurita, K., Sugita, K., Kodaira, N., Hirakawa, M., & Yang, J. (2005). Preparation and evaluation of trimethylsilylated chitin as a versatile precursor for facile chemical modifications. *Biomacromolecules*, *6*(3), 1414–1418.

Lee, S. B., Kim, I. H., Ryu, D. D. Y., & Taguchi, H. (1983). Structural properties of cellulose and cellulase reaction mechanism. *Biotechnology and Bioengineering*, *25*(1), 33–51.

Lefebvre, J., & Gray, D. (2005). AFM of adsorbed polyelectrolytes on cellulose I surfaces spin-coated on silicon wafers. *Cellulose*, *12*(2), 127–134.

Maren, R. (2009). . *Model cellulosic surfaces: History and recent advances. Model cellulosic surfaces* (vol. 1019) American Chemical Society.

Mi, F.-L., Shyu, S.-S., Lin, Y.-M., Wu, Y.-B., Peng, C.-K., & Tsai, Y.-H. (2003). Chitin/PLGA blend microspheres as a biodegradable drug delivery system: A new delivery system for protein. *Biomaterials*, *24*(27), 5023–5036.

Minke, R., & Blackwell, J. (1978). The structure of α-chitin. *Journal of Molecular Biology*, *120*(2), 167–181.

Montiel-González, Z., Luna-Bárcenas, G., & Mendoza-Galván, A. (2008). Thermal behaviour of chitosan and chitin thin films studied by spectroscopic ellipsometry. *Physica Status Solidi (C)*, *5*(5), 1434–1437.

Muzzarelli, R. A. (2011). Chitin nanostructures in living organisms. In N. S. Gupta (Ed.), *Chitin* (vol. 34) (pp. 1–34). The Netherlands: Springer.

Muzzarelli, R. A. A. (1980). Immobilization of enzymes on chitin and chitosan. *Enzyme and Microbial Technology*, *2*(3), 177–184.

Muzzarelli, R. A. A. (2009). Chitins and chitosans for the repair of wounded skin, nerve, cartilage and bone. *Carbohydrate Polymers*, *76*(2), 167–182.

Muzzarelli, R. A. A. (2012). Nanochitins and nanochitosans, paving the way to eco-friendly and energy-saving exploitation of marine resources. In M. Krzysztof, & M. Martin (Eds.), *Polymer science: A comprehensive reference* (pp. 153–164). Amsterdam: Elsevier BV.

Muzzarelli, R. A. A., Boudrant, J., Meyer, D., Manno, N., DeMarchis, M., & Paoletti, M. G. (2012). Current views on fungal chitin/chitosan, human chitinases, food preservation, glucans, pectins and inulin: A tribute to Henri Braconnot, precursor of the carbohydrate polymers science, on the chitin bicentennial. *Carbohydrate Polymers*, *87*(2), 995–1012.

Noh, H. K., Lee, S. W., Kim, J.-M., Oh, J.-E., Kim, K.-H., Chung, C.-P., et al. (2006). Electrospinning of chitin nanofibers: Degradation behavior and cellular response to normal human keratinocytes and fibroblasts. *Biomaterials*, *27*(21), 3934–3944.

Noishiki, Y., Takami, H., Nishiyama, Y., Wada, M., Okada, S., & Kuga, S. (2003). Alkali-induced conversion of β-chitin to α-chitin. *Biomacromolecules*, *4*(4), 896–899.

Ohashi, E., & Karube, I. (1995). Development of a thin membrane glucose sensor using β-type crystalline chitin for implantable biosensor. *Journal of Biotechnology*, *40*(1), 13–19.

Ohashi, E., & Koriyama, T. (1992). Simple and mild preparation of an enzyme-immobilized membrane for a biosensor using β-type crystalline chitin. *Analytica Chimica Acta*, *262*(1), 19–25.

Rejinold, N. S., Chennazhi, K. P., Tamura, H., Nair, S. V., & Rangasamy, J. (2011). Multifunctional chitin nanogels for simultaneous drug delivery, bioimaging, and biosensing. *ACS Applied Materials & Interfaces*, *3*(9), 3654–3665.

Rinaudo, M. (2006). Chitin and chitosan: Properties and applications. *Progress in Polymer Science*, *31*(7), 603–632.

Rudall, K. M., & Kenchington, W. (1973). The chitin system. *Biological Reviews*, *48*(4), 597–633.

Saito, Y., Okano, T., Gaill, F., Chanzy, H., & Putaux, J.-L. (2000). Structural data on the intra-crystalline swelling of β-chitin. *International Journal of Biological Macromolecules*, *28*(1), 81–88.

Saito, Y., Putaux, J. L., Okano, T., Gaill, F., & Chanzy, H. (1997). Structural aspects of the swelling of β chitin in HCl and its conversion into α chitin. *Macromolecules*, *30*(13), 3867–3873.

Sauerbrey, G. (1959). Verwendung von schwingquarzen zur wägung dünner schichten und zur mikrowägung. *Zeitschrift fur Physik*, *155*(2), 206–222.

Schaub, M., Wenz, G., Wegner, G., Stein, A., & Klemm, D. (1993). Ultrathin films of cellulose on silicon wafers. *Advanced Materials*, *5*(12), 919–922.

Schiffman, J. D., Stulga, L. A., & Schauer, C. L. (2009). Chitin and chitosan: Transformations due to the electrospinning process. *Polymer Engineering & Science*, *49*(10), 1918–1928.

Tzoumaki, M. V., Moschakis, T., & Biliaderis, C. G. (2010). Metastability of nematic gels made of aqueous chitin nanocrystal dispersions. *Biomacromolecules*, *11*(1), 175–181.

Wang, C., Kittle, J. D., Qian, C., Roman, M., & Esker, A. R. (2013). Chitinase activity on amorphous chitin thin films: A quartz crystal microbalance with dissipation monitoring and atomic force microscopy study. *Biomacromolecules*, *14*(8), 2622–2628.

Yokota, S., Kitaoka, T., Sugiyama, J., & Wariishi, H. (2007). Cellulose I nanolayers designed by self-assembly of its thiosemicarbazone on a gold substrate. *Advanced Materials*, *19*(20), 3368–3370.

Zeng, J.-B., He, Y.-S., Li, S.-L., & Wang, Y.-Z. (2012). Chitin whiskers: An overview. *Biomacromolecules*, *13*(1), 1–11.

Zhang, Y., Xue, C., Li, Z., Zhang, Y., & Fu, X. (2006). Preparation of half-deacetylated chitosan by forced penetration and its properties. *Carbohydrate Polymers*, *65*(3), 229–234.